Characterization of self-organized osteocytic spheroids using mouse osteoblast-like cells

Jeonghyun KIM*, Hiroyuki KIGAMI** and Taiji ADACHI*, **
*Institute for Frontier Life and Medical Sciences, Kyoto University
53 Shogoin-Kawahara-cho, Sakyo, Kyoto 606-8507, Japan
E-mail: adachi@infront.kyoto-u.ac.jp
**Department of Micro Engineering, Graduate School of Engineering, Kyoto University
53 Shogoin-Kawahara-cho, Sakyo, Kyoto 606-8507, Japan

Received: X January 2017; Revised: X February 2017; Accepted: X March 2017

Abstract
Osteocyte plays a central role as a commander in the bone to modulate bone remodeling processes. While the osteocyte is known to be differentiated from osteoblasts, understanding in mechanism of the osteocyte differentiation remained still poor. The aim of this study is to elucidate the osteocyte differentiation capability using three-dimensional (3D) cell culture technique. We first fabricated a self-organized spheroid reconstructed by mouse osteoblast-like cells by adjusting the number of subcultured cells in the round-bottom well. Compared to a conventional two-dimensional (2D) monolayer model, the 3D spheroid exerted greater osteocyte gene expressions *in vitro* within 2 days. As a result of the size-dependent experiment, there might be an appropriate cell-cell and cell-ECM interaction for osteoblast-like cells to induce the osteocytogenesis in the form of 3D spheroid culture. Moreover, the present model showed that the spheroid further exerted the prolonged osteocyte differentiation capability after a long period of incubation, 7 days. In conclusion, we characterized the self-organized osteocytic spheroids reconstructed by osteoblast-like cells and further suggested the potential application of the spheroid as a new *in vitro* tissue-engineered osteocytic model.

Keywords : Bone, Osteocytes, Differentiation, Osteoblast-like cells, Spheroid, Three-dimensional cell culture

1. Introduction

Three-dimensional (3D) culture system such as organoids has broadened our insight into understanding the human development or disease in many organs (Eiraku et al., 2011; Rossi, Manfrin and Lutolf, 2018). By providing an appropriate cellular culture environment as *in vivo* condition, the cells in the 3D culture system has enabled to recapitulate the structure or function of organs beyond a conventional two-dimensional (2D) *in vitro* system culturing cells on a stiff plastic or glass dish. Moreover, many researchers have also developed various 3D scaffold-free models using tissue-engineered techniques (Furukawa et al., 2003; Furukawa et al., 2008; Shimomura et al., 2018). Since the scaffold-free tissue was fabricated by collecting cells as spheroid or cell-sheet type without recruiting the artificial materials, the cells were surrounded by sufficient extracellular matrix (ECM) secreted from the surrounding cells, so that the scaffold-free models are expected to apply for an *in vitro* model and further for regenerative medicine.

As a commander in the bone, osteocytes embedded three-dimensionally inside the mineralized bone matrix play a central role to modulate bone remodeling processes by controlling osteoclasts and osteoblasts for bone resorption and formation, respectively (Bonewald, 2006; Adachi et al., 2009). While the osteocyte is known to be differentiated from the osteoblast cells, there is an insufficient understanding in mechanism of the osteocyte differentiation. In the previous study, our group first reported that cell condensation achieved by the 3D culture system triggers the osteocyte differentiation of osteoblast-like cells (Kim and Adachi, 2019).

Using a rotatory culture system, our group developed the fabrication method to mass-produce random heterogenous sizes (diameter: 50 – 250 μm) of spheroids reconstructed by the osteoblast-like cells (Kim and Adachi, 2019). While we revealed that the entire group of spheroids with heterogenous sizes induced the greater osteocyte differentiation capability

compared to the 2D monolayer condition, the size-dependent osteocyte differentiation capability of the spheroids remained unknown. Since the different sizes of 3D spheroid structure have different level of cell-cell and cell-extracellular matrix (ECM) interaction, it eventually induces an alteration in gradient generation for nutrients and gasses followed by distinct changes in the cell proliferation or function (Cui et al, 2017). Hence, a clear understanding in the effect of spheroid size on the differentiation capability is required. In this study, we attempted to establish the fabrication method of self-organized spheroid using the mouse osteoblast-like cells. Furthermore, we characterized and evaluated the spheroids in terms of a size- and time-dependent osteocyte differentiation manner.

2. Materials and method

2.1 Cell culture

In this study, we utilized the mouse osteoblast-like cell line, MC3T3-E1. The MC3T3-E1 cells have been widely utilized for *in vitro* study on the bone research including osteoblasts and osteocytes (Sato et al, 2006; Mullen et al, 2013). The cells were cultured in the α-MEM medium (Gibco) supplemented with 10% fetal bovine serum (Gibco) and 1% antibiotic-antimycotic (Gibco) in a humidified incubator at 37 °C with 5% CO_2. In this study, osteogenic supplements were not added in the culture medium. The cell passage was carried out when the cell confluency reached up to 80 – 90%. When preparing for 2D monolayer samples, 200,000 cells (cell density: 208 cells/mm^2) were seeded onto 35 mm petri dishes to become fully confluent after 2 days of culture.

2.2 Fabrication of spheroid

The spheroid was prepared in Nunclon Sphera 96-well round-bottom plate (Nalgene). To fabricate a desired size of the spheroid, we subcultured the certain number of cells in the round-bottom plate, such as 1,000, 2,500, 5,000, and 10,000 cells. Then, the incubation period for the spheroids varied from 1, 2, to 7 days depending on the aim of the experiment. The osteogenic supplements were not added during the fabrication process.

2.3 Real-time PCR

The spheroids were collected and washed with PBS. After removing the PBS by centrifugation, 1 ml of Isogen II (Nippon Gene) were added to lyse the sample. We then added 50 μl of p-Bromoanisole (Nacalai Tesque) into the sample in the Isogen II and mixed the sample gently. After the samples were centrifuged at 12,000 g for 10 minutes at 4 °C, a certain amount of transparent supernatant was separated from the mixture and reacted with the same amount of 70% ethanol. After reacting the mixture for 1 – 2 minutes, the mixtures were transferred into the spin cartridge (PureLink RNA Mini kit; Invitrogen). The spin cartridge was then centrifuged at 12,000 g for 15 seconds at 4 °C. According to the manufacturer's protocol, we carried out the washing process to purify and extract the RNA from the sample by dissolving in the RNase free water. By using the Transcriptor Universal cDNA Master (Roche) and PowerUp SYBR Green Master mix (ThermoFisher), we synthesized cDNA and performed real-time PCR, respectively. To examine the differentiation markers for osteoblasts, we examined the mRNA expression of runt-related transcription factor 2 (*Runx2*), alkaline phosphatase (*Alp*), and collagen, type I, alpha 1 chain (*Col1a1*). For osteocyte markers, we utilized osteopontin (*Opn*), the dentin matrix protein 1 (*Dmp1*), and sclerostin (*Sost*). The mRNA expressions were normalized to those of a reference gene, glyceraldehyde-phosphate dehydrogenase (*Gapdh*). All the genes were classified as previous study while the sets of gene-specific oligonucleotide primers were as described in Table. 1 (Bonewald, 2011).

Table 1. Primer List

Gene	Forward primer	Reverse primer	Amplicon size (bp)
Gapdh	TGTTCCTACCCCCAATGTGT	GGTCCTCAGTGTAGCCCAAG	137
Runx2	CAGTCCCAACTTCCTGTGCT	TACCTCTCCGAGGGCTACAA	94
Alp	GCTGATCATTCCCACGTTTT	ACCATATAGGATGGCCGTGA	120
Col1a1	CGTGCAATGCAATGAAGAAC	TCCCTCGACTCCTACATCTTCT	118
Opn	CCCGGTGAAAGTGACTGATT	GGCTTTCATTGGAATTGCTT	191
Dmp1	GGTTTTGACCTTGTGGGAAA	AATCACCCGTCCTCTCTTCA	91
Sost	CGTGCCTCATCTGCCTACTT	ATAGGGATGGTGGGGAGGT	185

[DOI: 10.1299/xxx.2017xxx000x]

2.4 Cell viability

The cell viability test was carried out by Double staining kit (Dojindo) containing Calcein-AM and Propidium Iodide (PI). After the spheroids were cultured for 2 or 7 days, the samples were collected in PBS. According to the manufacturer's protocol, the staining solution was prepared and added to the sample immersed in the PBS. The sample in the mixture was then incubated for 15 minutes at 37 °C. After incubation, the samples were observed using an excitation filter at 488 nm (live cells) and 546 nm (dead cells) by the FLUOVIEW FV3000 (Olympus).

2.5 Immunostaining

The spheroid was collected and fixed in the 4% paraformaldehyde (PFA). After rinsing with PBS, the sample was subjected to permeabilization for 30 minutes using 0.1% Triton-X. Then, the sample was treated with 3% bovine serum albumin (BSA) at room temperature for 1 hour, followed by treating with the anti-DMP1 antibody (Abcam) at room temperature for 1 hour. After washing twice with PBS, the samples were stained with the Alexa Flour 488 secondary antibody (Invitrogen), Alexa Fluor 546 Phalloidin (Invitrogen), and DAPI (Sigma) at room temperature for 1 hour. The stained samples were observed by the FLUOVIEW FV3000 (Olympus).

2.6 Statistical analysis

All bars in the real-time PCR results represent the means ± standard error. To evaluate the statistical significance of the observed differences, we carried out either Student's t-test or One-way ANOVA with Fisher's least significant difference (LSD) *post-hoc* test (with $\alpha = 0.05$). If a p-value obtained by the statistical analysis is less than 0.05, we assumed that the difference was significant.

3. Results

3.1 Self-organized spheroids were successfully fabricated by adjusting the number of subcultured cells

In this study, we fabricated the spheroid reconstructed by mouse osteoblast-like cells using a round-bottom plate. The sizes of spheroids were modulated by changing the number of cells subcultured in the round-bottom plate. By subculturing 1,000, 2,500, 5,000, and 10,000 cells as represented in Fig. 1(A), the average diameter of the spheroid at day 1 incubation were 149, 183, 243, and 307 μm, respectively. After 2 days incubation of the spheroid, the average diameter reduced to 115, 157, 193, and 234 μm, respectively. Moreover, the changes in the projected area of spheroid at day 2 compared to day 1 were 68.1% (Day 1: 13.6×10^3 μm^2, Day 2: 9.3×10^3 μm^2), 72.3% (Day 1: 23.4×10^3 μm^2, Day 2: 16.9×10^3 μm^2), 64.9% (Day 1: 41.8×10^3 μm^2, Day 2: 27.2×10^3 μm^2), and 62.9% (Day 1: 63.4×10^3 μm^2, Day 2: 39.9×10^3 μm^2). As represented in Figs. 1(B) and (C), using 1,000 cells and 10,000 cells, we fabricated the self-organized spheroids by culturing for 2 days.

After 2 days of incubation, we examined the cell viability of the spheroids reconstructed by 1,000 cells (sph1,000) and 10,000 cells (sph10,000) with the confocal fluorescence microscopy in Fig. 1(D), respectively. In the sph1,000, some of the dead cells (stained red) were found inside and outside of the spheroid while the population of live cells (stained green) occupied most of the part. Similarly, the sph10,000 also exhibited a few dead cells in the spheroid, but most of the part were live cells.

3.2 Spheroid reconstructed by 1,000 cells exerted the greater osteocyte gene expressions than that of 10,000 cells

To evaluate gene expression changes in the two types of spheroids (sph1,000 and sph10,000) after 2 days of incubation, we conducted real-time PCR in Fig. 2. Compared to the monolayer condition, mRNA expressions of osteoblast markers (*Runx2*, *Alp*, and *Col1a1*) and osteocyte markers (*Opn*, *Dmp1*, and *Sost*) in the sph1,000 were significantly up-regulated in 2 days; *Runx2* (3.06-fold change), *Alp* (4.27-fold change), *Col1a1* (3.52-fold change), *Opn* (56.9-fold change), *Dmp1* (1,266-fold change), and *Sost* (81.6-fold change). Similarly, the relative mRNA expressions in the sph10,000 to the monolayer were also entirely up-regulated while the change in *Col1a1* expression was a non-significant up-regulation. However, the relative mRNA expression changes in the sph10,000 to the monolayer were less than those in the sph1,000; *Runx2* (2.13-fold change), *Alp* (4.58-fold change), *Col1a1* (2.14-fold change), *Opn* (27.9-fold change), *Dmp1* (309-fold change), and *Sost* (73.2-fold change).

[DOI: 10.1299/xxx.2017xxx000x]

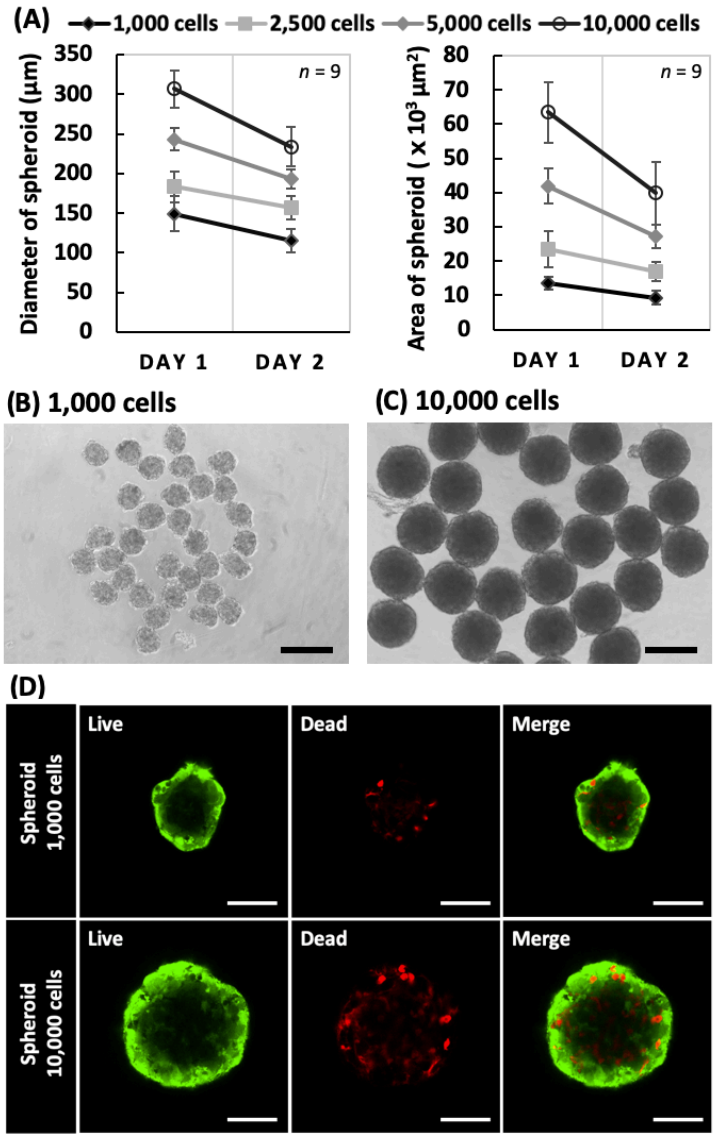

Fig. 1 (A) Average diameter and projected area of spheroids reconstructed by 1,000, 2,500, 5,000, 10,000 of mouse pre-osteoblast cells (n = 9). Spheroids reconstructed by (B) 1,000 and (C) 10,000 cells at day 2. Black bars represent 200 μm. (D) Cell viability test of spheroid reconstructed by 1,000 cells and 10,000 cells. Green and red indicate live and dead cells, respectively. White bars represent 50 μm.

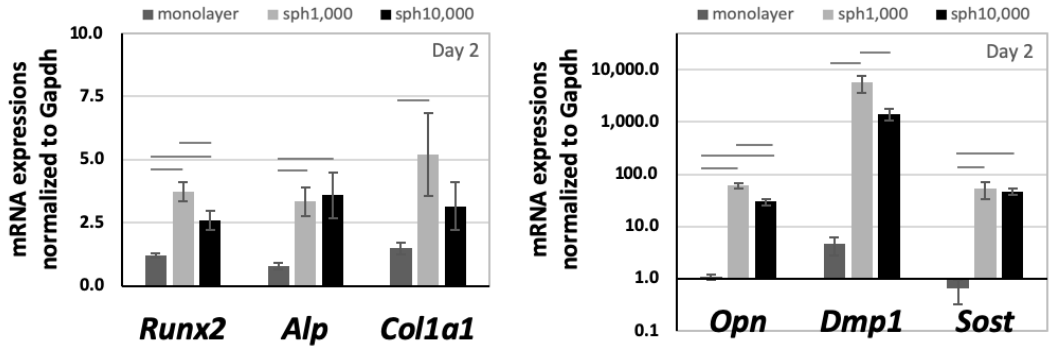

Fig. 2 mRNA expressions of osteoblast markers (*Runx2*, *Alp*, and *Col1a1*) and osteocyte markers (*Opn*, *Dmp1*, and *Sost*) in monolayer and spheroids reconstructed by 1,000 cells (sph1,000) and 10,000 cells (sph10,000) after 2 days of incubation. mRNA expression of all the genes were analyzed by real-time PCR and normalized by *Gapdh* expression. The bars represent the mean ± standard error (n = 4; bar indicates the significance between the groups, which was derived via one-way ANOVA with Fisher's LSD *post-hoc* test; α = 0.05)

[DOI: 10.1299/xxx.2017xxx000x]

3.3 Osteocyte gene and protein expressions were prolonged after 7 days of incubation.

Since the sph1,000 exerted the greater osteocyte gene expression at day 2 than the sph10,000, we carried out a longer period of experiment, 7 days, using the sph1,000. The gene expression changes of sph1,000 at 2-day and 7-day were measured by real-time PCR in Fig. 3(A). The 7-day incubation of spheroid significantly up-regulated the osteoblast gene expressions compared to the 2-day spheroid; *Runx2* (2.54-fold change; $p < 0.05$), *Alp* (12.1-fold change; $p < 0.05$), and *Col1a1* (2.43-fold change; $p < 0.05$). Furthermore, the spheroid cultured for 7 days also rendered the greater osteocyte gene expressions; *Opn* (1.41-fold change; $p = 0.07$), *Dmp1* (1.64-fold change; $p < 0.05$), and *Sost* (5.77-fold change; $p < 0.05$). In Fig. 3(B), we then conducted the immunostaining for the spheroid to examine the expression of DMP1 which is an osteocyte-specific marker. In 2-day incubation, the DMP1 was entirely expressed inside the spheroid. Moreover, the DMP1 expression was also prolonged in the spheroid after 7-day incubation.

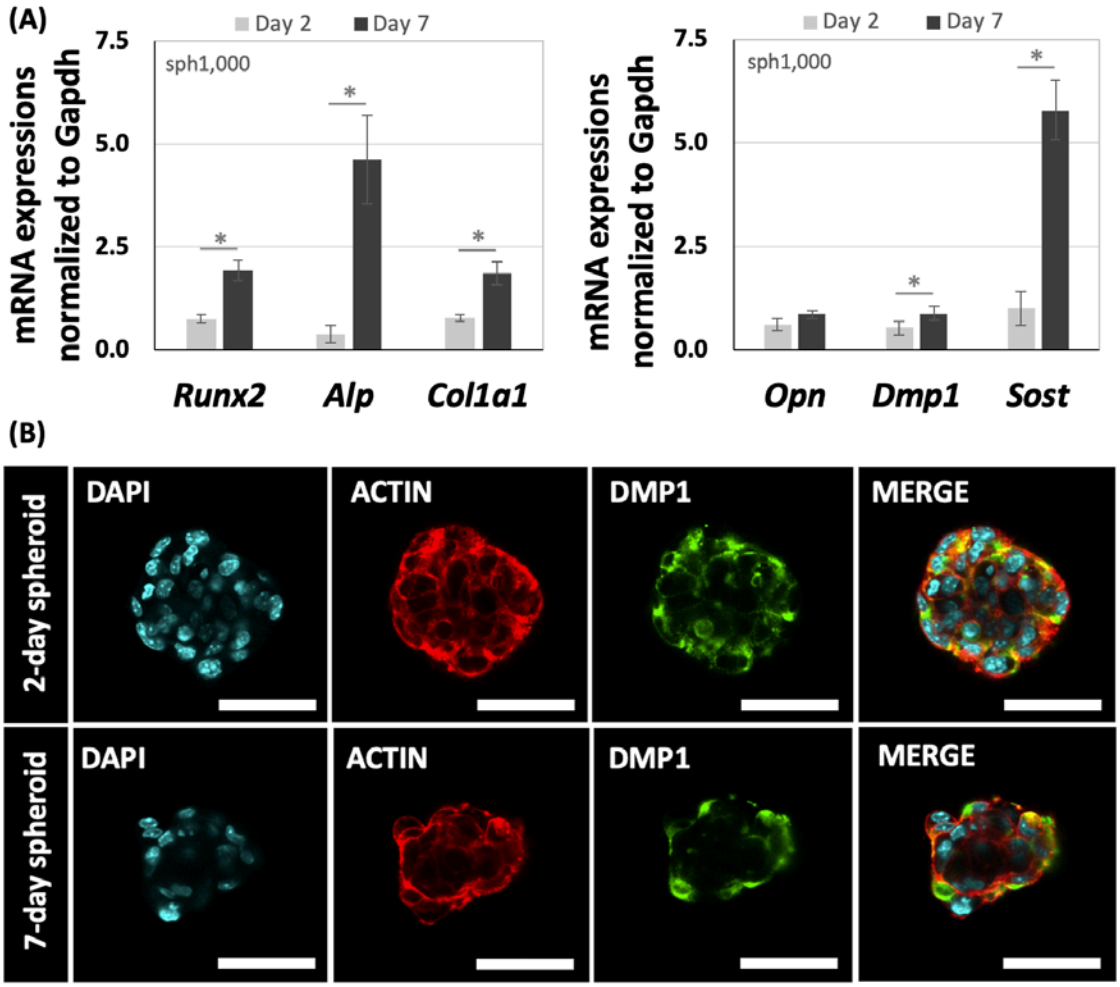

Fig. 3 (A) mRNA expressions of osteoblast markers (*Runx2*, *Alp*, and *Col1a1*) and osteocyte markers (*Opn*, *Dmp1*, and *Sost*) in spheroids reconstructed by 1,000 cells after 2 and 7 days of incubation. mRNA expression of all the genes were analyzed by real-time PCR and normalized to *Gapdh* expression. The bars represent the mean ± standard error ($n = 4$; p-value was obtained from Student's t-test; * $p < 0.05$). (B) Immunofluorescence staining images of 2-day and 7-day spheroid (sph1,000). The spheroids were stained with: DAPI (blue), ACTIN (red), and DMP1 (green). All experiments were independently repeated three times. White bar represents 50 μm.

4. Discussion

While several studies reported the effect of 3D culture system for osteoblasts on bone mineralization (Ferrera et al., 2002; Jähn, Richards, Archer and Stoddart, 2010), its effect on osteocyte differentiation remained unclear. In previous study, our group enabled mass production of spheroids with heterogenous sizes using the rotational culture system (Kim and Adachi, 2019). We showed that the spheroids reconstructed by mouse osteoblast-like cells exerted the osteocyte-

[DOI: 10.1299/xxx.2017xxx000x]

likeness *in vitro* within 2 days. The method using the rotational culture system, however, randomly fabricated the heterogeneous size of spheroids and was not capable of controlling the size of the spheroid. Since the different size of the 3D spheroid structure can be one of factors to alter the level of differentiation capability, we explored the size-dependent osteocyte differentiation capability of the osteoblast-like cells. In this study, we utilized the round-bottom plate with the super low cell attachment surface. By altering the number of the cells (1,000, 2,500, 5,000, and 10,000 cells) subcultured in the round-bottom plate, it allowed to fabricate a desired diameter of the spheroid after 2 days of cultivation.

During the fabrication of spheroid by adjusting the number of subcultured cells, we reported the size reduction from 1-day to 2-day incubation. The size change in spheroids were thought to be due to strengthening cell-cell interaction in the 3D spheroid as the cultivation time passed. In addition, microarray data in the previous study represented that the proliferation-related gene expressions for the spheroid were significantly suppressed compared to the 2D condition on the culture dish (Kim and Adachi, 2019). It implies that the proliferation of the cells in the 3D spheroid stopped while it induced the osteocyte differentiation. Two different size of sph1,000 and sph10,000 represented living cells for the most of the part while a few dead cells were also exhibited. Especially, the sph10,000 tends to have a slightly more population of dead cells due to a lack of oxygen and nutrients diffusion reached as the spheroid size become greater (Oh et al, 2009; Chung and King, 2011). Moreover, the number of dead cells in the sph10,000 compared to the sph1,000 was increased because the total number of cells in the sph10,000 was simply greater than that of sph1,000.

As a result of real-time PCR and immunostaining, the spheroids reconstructed by osteoblast-like cells exerted osteocyte-likeness *in vitro* within 2 days. The result corresponds to the previous study using the rotational culture system. From the previous study, we suggested that the cell condensation achieved in the 3D culture system led to the osteocyte differentiation, but the detailed driving factor induced by the cell condensation remained unknown. In order to understand this uncleared mechanism, we fabricated different sizes of spheroids and evaluated their gene expressions in those spheroids which were subjected to relative changes in the level of cell-cell interaction, cell-ECM interaction, and hypoxia. The cell-cell and cell-ECM interaction were strengthened as the size of spheroid become larger (Gong et al, 2015), but the greater cell-cell and cell-ECM interaction in the sph10,000 did not promote the osteocyte gene expressions compared to the sph1,000. Consequently, it may have an appropriate cell-cell and cell-ECM interaction for the osteoblast-like cells to induce the osteocytogenesis in the 3D structure. Similarly, a greater hypoxic condition is applied to the cells inside the spheroid compared to the surface of the spheroid, and the hypoxic condition also becomes greater as the size of spheroid increases (Nunes et al, 2019). While the cells inside the sph1,000 were exposed to a relatively less hypoxia than the sph10,000, the osteocyte gene expressions in the sph1,000 were greater than that in the spher10,000. Hence, the hypoxia in the spheroid did not greatly contribute to the up-regulations in osteocyte gene expressions of osteoblast-like cells. On the other hand, the osteoblast-like cells cultured in 2D monolayer may not be the appropriate condition to induce the osteocyte differentiation, but osteoblast differentiation. While many groups have attempted to evoke the osteocyte differentiation using the chemical induction by osteogenesis supplements on the 2D culture dish, it took such a long period of cultivation, several weeks to months (Bhargava et al, 1988; Franz-Odendaal et al, 2006; Uchihashi et al, 2013), which is not an efficient model to study cellular differentiation. Our findings might imply that it is essential for the osteocyte differentiation of the osteoblast-like cells to require a certain cellular environment where the osteoblast cells encounter the appropriate cell-cell and cell-ECM interaction as *in vivo* processes such as unmineralized bone matrix termed osteoid. Further study will be required to characterize the cellular environment in the spheroid with regard to its ECM accumulation and also to elucidate the detailed mechanism of signal-transduction pathways for the osteocyte differentiation achieved in the 3D culture system.

Since the sph1,000 exerted the greater osteocyte differentiation capability compared to the sph10,000 or monolayer reconstructed by the osteoblast-like cells, the sph1,000 was utilized for 7 days of the long incubation experiment in Fig. 3. The previous model could not undergo the longer period of experiment than 2 days because each of the spheroids in the culture dish become attached and expanded (Kim and Adachi, 2019). On the other hand, each one of the present models allowed to cultivate inside an independent well for a longer period. By conducting the long period of cultivation experiment targeting the single spheroid, we first exhibited up-regulations of both osteoblast and osteocyte gene expressions after 7 days of cultivation experiment. Especially, the mature osteocyte marker, *Sost*, was significantly and remarkably up-regulated compared to the spheroid incubated for 2 days. The size of 7-day spheroid was reduced while the real-time PCR and immunostaining results represented that the spheroid still rendered the osteocyte-likeness. The results altogether imply that the spheroid reconstructed by osteoblast-like cells did not only trigger the osteocyte differentiation within 2 days, but it prolonged the osteocyte-likeness for 7 days. It is such a remarkable outcome achieved

[DOI: 10.1299/xxx.2017xxx000x]

without any chemical inductions such as osteogenic supplements. Further study using the primary cells will be needed to support our findings for utilization of our present model as a new *in vitro* tissue-engineered osteocytic model.

5. Conclusion

In this study, we successfully developed the self-organized and size-controlled spheroid using osteoblast-like cells to represent the osteocyte-likeness *in vitro*. We then evaluated the size-dependent osteocyte differentiation capability and showed that the sph1,000 rendered the greater gene expressions in the osteocyte markers than sph10,000 or monolayer. This may imply that the mouse osteoblast-like cells have a preferred cell-cell and cell-ECM interaction for osteocytogenesis in the 3D spheroid. Moreover, we first reported that the spheroid is capable of prolonging the osteocyte-likeness for 7 days by *in vitro* cultivation. Hereby, we suggest the potential application of the spheroid using osteoblast-like cells as a new *in vitro* osteocytic model.

Acknowledgement

We would like to appreciate Junko Sunaga for providing technical advices. This work was supported by Advanced Research and Development Programs for Medical Innovation (AMED-CREST), by elucidation of mechanobiological mechanisms and their application to the development of innovative medical instruments and technologies from Japan Agency for Medical Research and Development (AMED) (JP20gm0810003), by the acceleration program for intractable diseases research utilizing disease-specific iPS cells from AMED (JP19bm0804006), and by the Japan Society for the Promotion of Science (JSPS) KAKENHI (20H00659, 20K20181, and 19K23604).

References

Adachi, T., Aonuma, Y., Ito, S., Tanaka, M., Hojo, M., Takano-Yamamoto, T. and Kamioka, H., Osteocyte calcium signaling response to bone matrix deformation, Journal of Biomechanics, Vol.42, No.15 (2009) pp.2507–2512, DOI: 10.1016/j.jbiomech.2009.07.006

Bhargava, U., Bar-Lev, M., Bellows, C. G. and Aubin, J. E., Ultrastructural analysis of bone nodules formed in vitro by isolated fetal rat calvaria cells, Bone, Vol.9 (1988) pp.155–163, DOI: 10.1016/8756-3282(88)90005-1

Bonewald, L. F., Mechanosensation and transduction in osteocytes, BoneKEy-Osteovision, Vol.3, No.10 (2006) pp.7–15, DOI: 10.1138/20060233

Bonewald, L. F., The amazing osteocyte, Journal of Bone and Mineral Research, Vol.26, No.2 (2011) pp.229–238, DOI: 10.1002/jbmr.320

Chung, S. and King, M. W., Design concepts and strategies for tissue engineering scaffolds, Biotechnology and Applied Biochemistry, Vol.58, No.6 (2011) pp.423–438, DOI: 10.1002/bab.60

Cui, X., Hartanto, Y. and Zhang, H., Advances in multicellular spheroids formation, Journal of the Royal Society Interface, 14: 20160877 (2017), DOI: 10.1098/rsif.2016.0877

Eiraku, M., Takata, N., Ishibashi, H., Kawada, M., Sakakura, E., Okuda, S., Sekiguchi, K., Adachi, T. and Sasai, Y., Self-organizing optic-cup morphogenesis in three-dimensional culture, Nature, Vol.472, No.7341 (2011) pp.51–56, DOI: 10.1038/nature09941

Ferrera, D., Poggi, S., Biassoni, C., Dickson, G. R., Astigiano, S., Barbieri, O., Favre A., Franzi A., Strangio A. and Manduca, P., Three-dimensional cultures of normal human osteoblasts: Proliferation and differentiation potential in vitro and upon ectopic implantation in nude mice. Bone. Vol.30, No.5 (2002) pp.718-725, DOI: 10.1016/s8756-3282(02)00691-9

Franz-Odendaal, T. A., Hall, B. K. and Witten, P. E., Buried alive: How osteoblasts become osteocytes, Developmental Dynamics, Vol.235 (2006) pp.176–190, DOI: 10.1002/dvdy.20603

Furukawa, K. S., Imura, K., Tateishi, T. and Ushida, T. Scaffold-free cartilage by rotational culture for tissue engineering, Journal of Biotechnology, Vol.133, No.1 (2008) pp.134–145, DOI: 10.1016/j.jbiotec.2007.07.957

Furukawa, K. S., Suenaga, H., Toita, K., Numata, A., Tanaka, J., Ushida, T., Sakai, Y. and Tateishi, T., Rapid and large-scale formation of chondrocyte aggregates by rotational culture, Cell Transplantation, Vol.12, No.5 (2003) pp.475–479, DOI: 10.3727/000000003108747037

Gong, X., Lin, C., Cheng, J., Su, J., Zhao, H., Liu, T., Wen X. and Zhao, P., Generation of multicellular tumor spheroids with microwell-based agarose scaffolds for drug testing, PLoS ONE, Vol.10, No.6 (2015), DOI:10.1371/journal.pone.0130348.

[DOI: 10.1299/xxx.2017xxx000x]

Jähn, K., Richards, R. G., Archer, C. W. and Stoddart, M. J., Pellet culture model for human primary osteoblasts. European Cells and Materials, Vol.20, (2010) pp.149-161, DOI: 10.22203/ecm.v020a13

Kim, J. and Adachi, T., Cell condensation triggers the differentiation of osteoblast precursor cells to osteocyte-like cells, Frontiers in Bioengineering and Biotechnology, Vol.7, No.288 (2019), DOI: 10.3389/fbioe.2019.00288

Mullen, C. A., Haugh, M. G., Schaffler, M. B., Majeska, R. J. and McNamara, L. M., Osteocyte differentiation is regulated by extracellular matrix stiffness and intercellular separation, Journal of the Mechanical Behavior of Biomedical Materials. Vol.28 (2013) pp.183-194, DOI: 10.1016/j.jmbbm.2013.06.013

Nunes, A. S., Barros, A. S., Costa, E. C., Moreira, A. F. and Correia, I. J., 3D tumor spheroids as in vitro models to mimic in vivo human solid tumors resistance to therapeutic drugs, Biotechnology and Bioengineering, Vol.116, No.1 (2019) pp.206-226, DOI: 10.1002/bit.26845

Oh, S. H., Ward, C. L., Atala, A., Yoo, J. J. and Harrison, B. S., Oxygen generating scaffolds for enhancing engineered tissue survival, Biomaterials, Vol.30, No.5 (2009) pp.757–762, DOI: 10.1016/j.biomaterials.2008.09.065

Rossi, G., Manfrin, A. and Lutolf, M. P., Progress and potential in organoid research, Nature Reviews Genetics, Vol.19 (2018) pp.671–687, DOI: 10.1038/s41576-018-0051-9

Sato, K., Adachi, T., Shirai, Y., Saito, N. and Tomita, Y., Local disassebly of actin stress fibers induced by selected release of intracellular tension in osteoblastic cell, Journal of Biomechanical Science and Engineering, Vol.1, No.1 (2006) pp.204–214, DOI: 10.1299/jbse.1.204

Shimomura, K., Ando, W., Fujie, H., Hart, D. A., Yoshikawa, H. and Nakamura, N., Scaffold-free tissue engineering for injured joint surface restoration, Journal of Experimental Orthopaedics, Vol.5, No.2 (2018), DOI: 10.1186/s40634-017-0118-0

Uchihashi, K., Aoki, S., Matsunobu, A. and Toda, S., Osteoblast migration into type I collagen gel and differentiation to osteocyte-like cells within a self-produced mineralized matrix: A novel system for analyzing differentiation from osteoblast to osteocyte. Bone, Vol.52 (2013) pp.102–110, DOI: 10.1016/j.bone.2012.09.001

[DOI: 10.1299/xxx.2017xxx000x]